# Non-Stationary CT Image Noise Spectrum Analysis

Michael Balda[1], Björn J. Heismann[1,2], Joachim Hornegger[1]

[1]Pattern Recognition Lab, Friedrich-Alexander-Universität Erlangen
[2]Siemens Healthcare, Erlangen
michael.balda@informatik.uni-erlangen.de

**Abstract.** We investigate the spatial dependency of noise characteristics in CT images. The perceived image quality depends on the noise-granularity. Especially in low-dose applications the noise granularity influences the diagnostic value. A model is presented, that provides two-dimensional, stationary noise realizations for arbitrary image pixel locations from which two-dimensional Noise Power Spectrum estimates can be computed. It fully incorporates the CT reconstruction process for (indirect) fan-beam reconstruction, the quarter offset of the detector channels and the detector noise characteristics. It can be used with simulated and measured data and allows for the assessment of spectral noise characteristics for arbitrary objects.

## 1 Introduction

The noise in the reconstructed CT image is influenced by various parameters. When planning components of a Computed Tomography scanner, like detectors or X-ray tubes, it is necessary to tune their parameters in a way that leads to the best achievable objective image quality. In terms of software aspects, different reconstruction techniques and several noise-reduction algorithms like sinogram pre-processing exist, which have to be evaluated not only in terms of total noise reduction but also on their influence on the image quality. These tasks require methods to assess the image noise characteristics.

Fig. 1 illustrates the typical noise characteristics of a CT image. The noise texture shows an isotropic grain structure at the center. Towards the boundary it decreases and becomes increasingly oriented. This effect can be observed in both images of different water phantoms. There are models which analytically compute the noise variance propagation for the inverse Radon transform [1], more precise noise propagation models also include local correlations introduced by various reconstruction steps [2]. Additionally, several approaches have been made, which model the noise propagation from the detector noise transfer function to the image noise power spectrum (NPS) [3], [4] but these models are limited by the fact, that the assumptions on the noise transfer functions (like detector- or focus-noise transfer function) are only valid for the image center. Objective quality measures of a CT image, however, rely on an assessment of the noise characteristics throughout the whole image.

## 2 Materials and Methods

We develop a model to generate two-dimensional realizations of the image noise and NPS estimates for arbitrary image positions. It uses a projection noise model. For any pixel position and projection angle, an ensemble of projection noise values at the associated detector position is generated. This local detector noise signal then undergoes all steps of the reconstruction algorithm that influence the noise characteristics. Back-projection of the according noise signals for each angle yields a stationary, two-dimensional noise realization for this image location. This model gives an insight into the noise shaping properties of the filtered back-projection (FBP). Unlike analytical noise propagation methods, it can be easily adapted to any FBP-based reconstruction algorithm and various effects can be incorporated into the model without greatly increasing its overall complexity.

The characteristics of this noise realization will differ throughout the image and resemble the CT image noise at a selected location $\boldsymbol{p} = (p_x, p_y)^T$. The value of an image pixel depends on the attenuation of all beams passing through this pixel. These beams have associated projection angles $\phi \in [0; \pi)$. The model creates a stationary local noise image patch $i_{\mathbf{p}}(\boldsymbol{x})$ using the following steps for all projection angles $\phi$ ([5] for a concise description of the FBP):

1. *Find measured attenuation value:* The detector coordinate $\gamma(\mathbf{p}, \phi)$ can be computed as follows:

$$\gamma(\mathbf{p}, \phi) = \left( \operatorname{atan2} \left( \frac{r(\mathbf{p}) \cdot \cos(\phi - \phi_T(\mathbf{p}))}{d_{\mathrm{SOC}} + r(\mathbf{p}) \cdot \sin(\phi - \phi_T(\mathbf{p}))} \right) + \frac{\beta}{2} - \beta_a \right) \cdot \frac{1}{\Delta\beta} \quad (1)$$

The complete fan angle is $\beta$, $\Delta\beta$ is the fan angle between two neighboring detector channels, $\beta_a$ is the alignment angle due to the quarter offset ($\beta_a = 0$ for no quarter offset). The distance between X-ray source and origin is denoted $d_{\mathrm{SOC}}$, the polar coordinates of $\boldsymbol{p}$ are denoted $r(\boldsymbol{p})$ for the distance to

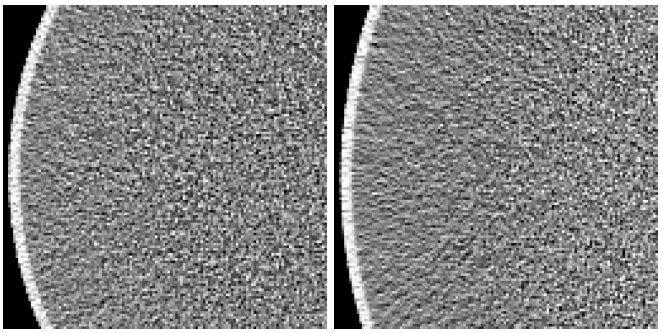

**Fig. 1.** Excerpts (125 mm×125 mm) of CT images of water phantoms: 300 mm diameter (left), 400 mm diameter (right).

the origin and $\phi_T(\mathbf{p})$ for the polar angle. Using $\gamma(\boldsymbol{p}, \phi)$, the according attenuation value $\mu(\gamma(\boldsymbol{p}, \phi), \phi)$ can be interpolated from the measured projection data.

2. *Initialize projection noise model:* The projection noise model provides a noise distribution for the attuenuation values $\mu(\gamma(\boldsymbol{p}, \phi), \phi)$. The noise in the attenuation values measured by the detector consists of electronics noise, quantization noise and quantum noise. The quantum noise depends on the number of incoming X-ray quanta. A detailed description on how quantum noise affects the detected attenuation values can be found in [1]. In practice, the noise effects can either be modeled or assessed by calibration measurements. Usually, the detector noise signal can be assumed to be uncorrelated and white. In practice minor correlations between the detector channels are introduced by optical cross-talk.
3. *Generate virtual detector noise signals:* A virtual, stationary detector noise signal is generated, that has constant noise distribution parameters throughout all channels. In case of rebinning to parallel beam geometry, an additional reading is generated with identical parameters. It represents the projection from the opposite direction. If the detector noise cross-talk behavior should be considered, these signals have to be convoluted with the impulse response of the detector.
4. *Rebin virtual noise signal:* The rebinning also influences the NPS. It consists of two steps. First the beams are reordered to parallel beam geometry with inhomogeneous ray distances. This requires a 2-D interpolation in the sinogram. In case of a quarter offset, the beams from opposite projection directions are then sorted into one single reading with the double amount of channels, finally the readings are resampled to homogeneous ray distances which requires a 1-D interpolation. In case of direct FBP, this step is omitted.
5. *Filtered back-projection:* The rebinned virtual noise signal is filtered and back-projected. The resulting noise pattern is stationary and resembles noise characteristics as this specific location in the image.

### 2.1 Algorithm

The algorithm can be summarized as follows.

1. Set projection angle $\phi = -\pi/2 + \Delta\phi \cdot r$ and $\Delta\phi = \pi/n_r$
2. Calculate $\gamma(\mathbf{x}, \phi)$ according to (1) and interpolate reading $d_\phi[c]$ at $\gamma$ to get attenuation value $\mu(\phi)$.
3. Initialize detector noise generator with $\mu(\phi)$.
4. Generate two vectors of noise signal realizations $\tilde{\boldsymbol{d}}_{n,i}[c]$ with $c \in [0; N_d]$ and $i \in \{1, 2\}$.
5. Perform rebinning on $\tilde{\boldsymbol{d}}_{n,1}$ and $\tilde{\boldsymbol{d}}_{n,2}[c]$ to get $\hat{\boldsymbol{d}}_n[c_p]$.
6. Back-project $\tilde{\boldsymbol{d}}_t[c_p]$ onto the noise patch $i_{\boldsymbol{x}}$.
7. if $r < N_r$: Set $r = r + 1$ and GOTO 2;

The length of the detector noise signal $N_d$ has to be chosen according to the desired size and field of view (FOV) of the noise resulting image patch $i_{\mathbf{x}}$ so that the image patch is fully covered by the back-projected values of $\tilde{\boldsymbol{d}}_t[c]$, $n_r$ is the number of desired rotation angle samples.

## 3 Results and Discussion

The algorithm was tested with several measured and simulated phantoms. Fig. 2(a) shows the reconstruction of a simulated phantom with marked voxel locations. This phantom is especially suited to demonstrate the properties of the proposed method, since the two strongly attenuating bone structures have a dominating influence on the noise structure of the whole image. Fig. 3 displays the respective stationary noise patches and the corresponding NPS estimates. Dominating noise components in directions of strong attenuation (between the two bones) can be observed. This leads to an increasingly directed noise grain structure. For the pixel close to the border, there is no such dominant influence on the noise direction, this leads to a more homogeneous noise structure. The overall noise is stronger for pixels close to the center and / or near strong attenuators. For testing the noise model on measured data, an elliptic water phantom of 450 mm width and 225 mm height was used. Fig. 2(b) shows the measured noise standard deviation from a circular ROI of radius 50 mm shifted along the longer axis of the ellipse. The corresponding model estimates are generated with the introduced method, an analytic forward projector and a calibrated noise model. The measurement and the values computed with the model on simulated data show a good agreement with relative deviations below 5 %.

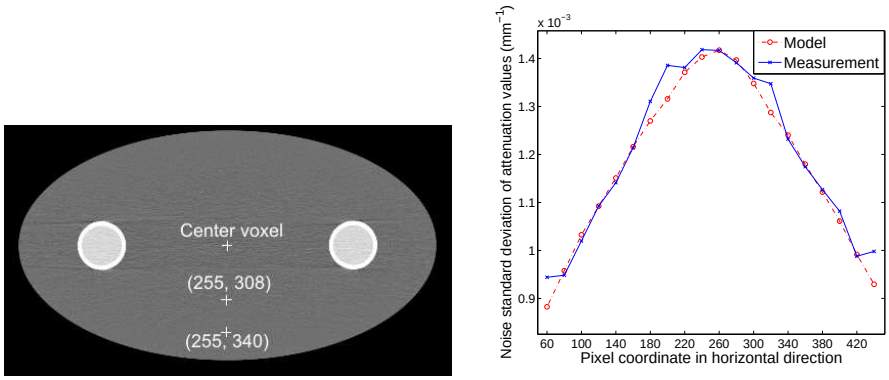


**Fig. 2.** Left: Reconstruction of an elliptical water phantom with two femur bone structures. Noise patches are provided in Fig. 3 for marked voxel locations; Right: Comparison of noise standard deviation in from measured data and model.

**Fig. 3.** Top row: Noise patches for voxels marked in Fig. 2(a) (window center: 0, width: 4.2 HU); bottom row: normalized NPS estimates computed from noise patches above.

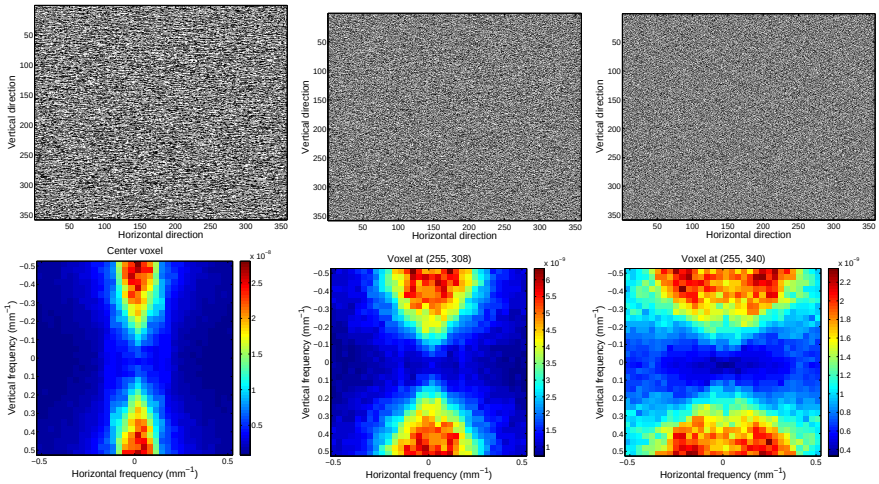


## 4 Conclusion

We have introduced a method to generate stationary noise patches and Noise Power Spectrum estimates that resemble the noise characteristics of arbitrary voxel positions of CT images. The NPS estimates show the influence of object structures and reconstruction properties on the image noise structures. The model can be easily adapted to various FBP-based reconstruction techniques. This method can be used as a valuable tool to evaluate the influence of reconstruction parameters such as reconstruction kernels or noise adapted sinogram-filters on the quality of the reconstructed image.

## References

1. Buzug TM. Einführung in die Computertomographie: Mathematisch-physikalische Grundlagen der Bildrekonstruktion. Berlin: Spinger; 2005.
2. Borsdorf A, Kappler S, Raupach R, et al. Analytic noise propagation for anisotriopic denoising of CT images. In: IEEE Nucl Sci Symp Conf Rec; 2008. p. 5335–38.
3. Riederer SJ, Pelc NJ, Chesler DA. The noise power spectrum in computed X-ray tomography. Phys Med Biol. 1978;23(3):446–54.
4. Kijewski MF, Judy PF. The noise power spectrum of CT images. Phys Med Biol. 1987;32(5):565–75.
5. Kak AC, Slaney M. Principles of Computerized Tomographic Imaging. Soc Ind Appl Math Publishing; 2001.